IceBridge Sander AIRGrav L4 Bathymetry, Version 1

USER GUIDE

How to Cite These Data

As a condition of using these data, you must include a citation:

Tinto, K., Bell, R. E., & Cochran, J. R. (2014, updated 2018). *IceBridge Sander AIRGrav L4 Bathymetry* (IGBTH4, Version 1) [Data set]. Boulder, Colorado USA. NASA National Snow and Ice Data Center Distributed Active Archive Center. https://doi.org/10.5067/DQVUVQCRYAM4 [Date Accessed].

FOR QUESTIONS ABOUT THESE DATA, CONTACT NSIDC@NSIDC.ORG

FOR CURRENT INFORMATION, VISIT https://nsidc.org/data/IGBTH4

National Snow and Ice Data Center

TABLE OF CONTENTS

1 DATA DESCRIPTION

1.1 Summary

This data set contains bathymetry of Arctic fjords and Antarctic ice shelves based on measurements from the Sander Geophysics Airborne Inertially Referenced Gravimeter (AIRGrav) system. The data were collected as part of Operation IceBridge funded aircraft survey campaigns.

1.2 Format

The data files are in CSV format with associated XML files that contain additional metadata.

1.3 File Naming Convention

The data files have the naming convention shown below. File name variables are described in Table 1.

IGBTH4_20140207.xyz
IGBTH4_20140207.csv
IGBTH4_20140207.csv.xml

Table 1. Bathymetry Profile Data File Naming Convention

Variable	Description
IGBTH4	File name prefix indicating Level-4 bathymetry data
YYYYMMDD	Four-digit year, two-digit month, and two-digit day of data delivery date
.xyz	Indicates ASCII .csv file or .xml file

1.4 File Size

The .csv files range from approximately 800 KB to 5 MB. The entire data set is approximately 11 MB.

1.5 Spatial Coverage

Spatial coverage for the IceBridge Sander AIRGrav L4 Bathymetry profiles data includes the Arctic and Antarctic areas listed below.

Greenland Profiles

Southernmost Latitude: 62° N

Northernmost Latitude: 83° N
Westernmost Longitude: 70° W
Easternmost Longitude: 17° W

Northwest Greenland Grid
Southernmost Latitude: 72° N
Northernmost Latitude: 77° N
Westernmost Longitude: 67° W
Easternmost Longitude: 50° W

Antarctica: Abbot Ice Shelf Profiles
Southernmost Latitude: 74° S
Northernmost Latitude: 72° S
Westernmost Longitude: 104° W
Easternmost Longitude: 90° W

1.5.1 Spatial Resolution

For Greenland data, fjords are commonly represented by a single profile with points at 500 m intervals. The along-track resolution of inverted gravity is ~4.4 km, corresponding to the 70 s filter and average survey speed of 125 m/s. Shorter wavelength features are from the radar-derived bed used to constrain the model. Profile lines approximate the fjord axis, but in parts were flown to the side of the midline and show shallower bathymetry corresponding to the fjord edges. Users are cautioned to check the flight track of profile data in order not to misinterpret this shallow bathymetry as an axial sill.

The northwest Greenland grid was flown at 5 km line spacing, with an average speed of 125 m/s giving an along-track resolution of 4.4 km. Data were gridded at 500 m cell size for inversion and then resampled along the flight lines.

The survey over Abbot Ice Shelf was flown as a series of nearly north-south parallel lines, 30 to 54 km apart (mean of 39.2 km), across the ice shelf and a single, nearly east-west line along the ice shelf axis. Free-air anomalies were filtered with a 70 s full wavelength filter, resulting in approximately 4.9 km half-wavelength resolution for a typical flying speed of 140 m/s (Cochran et al. 2014).

1.5.2 Projection and Grid Description

Greenland Profiles
Spacing: 500 m (point)

Projection: Polar Stereographic true at 70° N, origin 90° N, 45° W (EPSG 3413) bathymetry positive downward from WGS-84 ellipsoid.

Northwest Greenland Grid
Spacing: 500 m point spacing.

Projection: Polar Stereographic true at 70° N, origin 90° N, 45° W (EPSG 3413) bathymetry positive downward from WGS84 ellipsoid.

Antarctica: Abbot Ice Shelf Profiles
Spacing: 200 m (point)

Projection: Polar Stereographic true at 71° S, 0 up, 180 down, bathymetry positive downward from GLO4C geoid (Forste et al, 2008).

1.6 Temporal Coverage

1 January 2010 to 31 December 2016

1.6.1 Temporal Resolution

IceBridge campaigns were conducted annually. Arctic and Greenland campaigns were conducted during March, April, and May; and Antarctic campaigns were conducted during October and November.

1.7 Parameter or Variable

The IceBridge Sander AIRGrav L4 Bathymetry profiles data set contains profile lines, location in Polar Stereographic easting and northing, and bathymetry measured positively downwards.

1.7.1 Parameter Description

The bathymetry profile data file contains fields as described in Table 2. Profile data are preceded by a ten line header.

Table 2. Parameter Descriptions and Units

Column	Name	Description	Units
1	LINE	Greenland data: Line ID: XX.YYZ XX = Individual Glacier ID YY = Year of flight Z = Repeat tracks Abbot data: Line ID: abbotXX XX = line number	n/a
2	FAG070_mGal	Free Air Gravity Anomaly, measured	mGal
3	FAG_calc_mGal	Free Air Gravity anomaly, calculated	mGal
4	LON	Longitude on WGS84 ellipsoid	Degrees
5	LAT	Latitude on WGS84 ellipsoid	Degrees
6	X	X Coordinate (EPSG 3413)	Meters
7	Y	Y Coordinate (EPSG 3413)	Meters
8	BATHY_m	Modeled bathymetry from gravity inversion: positive down, with respect to WGS-84 ellipsoid	Meters

1.7.2 Sample Data Record

Figure 1 shows a portion of the IGBTH4_20140207.csv data file.

```
#LINE, FAG070_mGal, FAG_calc_mGal, LON, LAT, X, Y, BATHY_m
14.100, 49.4, 57.4, -49.195798, 71.541458, -147526, -2010937, 924
14.100, 49.4, 57.3, -49.197407, 71.541373, -147583, -2010942, 923
14.100, 49.4, 57.2, -49.199015, 71.541288, -147640, -2010947, 922
14.100, 49.4, 57.1, -49.200621, 71.541204, -147697, -2010952, 921
14.100, 49.4, 57.1, -49.202233, 71.541119, -147754, -2010958, 920
14.100, 49.4, 57, -49.203843, 71.541035, -147811, -2010963, 919
14.100, 49.4, 56.9, -49.205453, 71.540951, -147869, -2010968, 917
14.100, 49.4, 56.8, -49.207068, 71.540866, -147926, -2010973, 916
```

Figure 1. Sample data file (IGBTH4_20140207.csv)

Figure 2 shows the locations of the Greenland profiles.

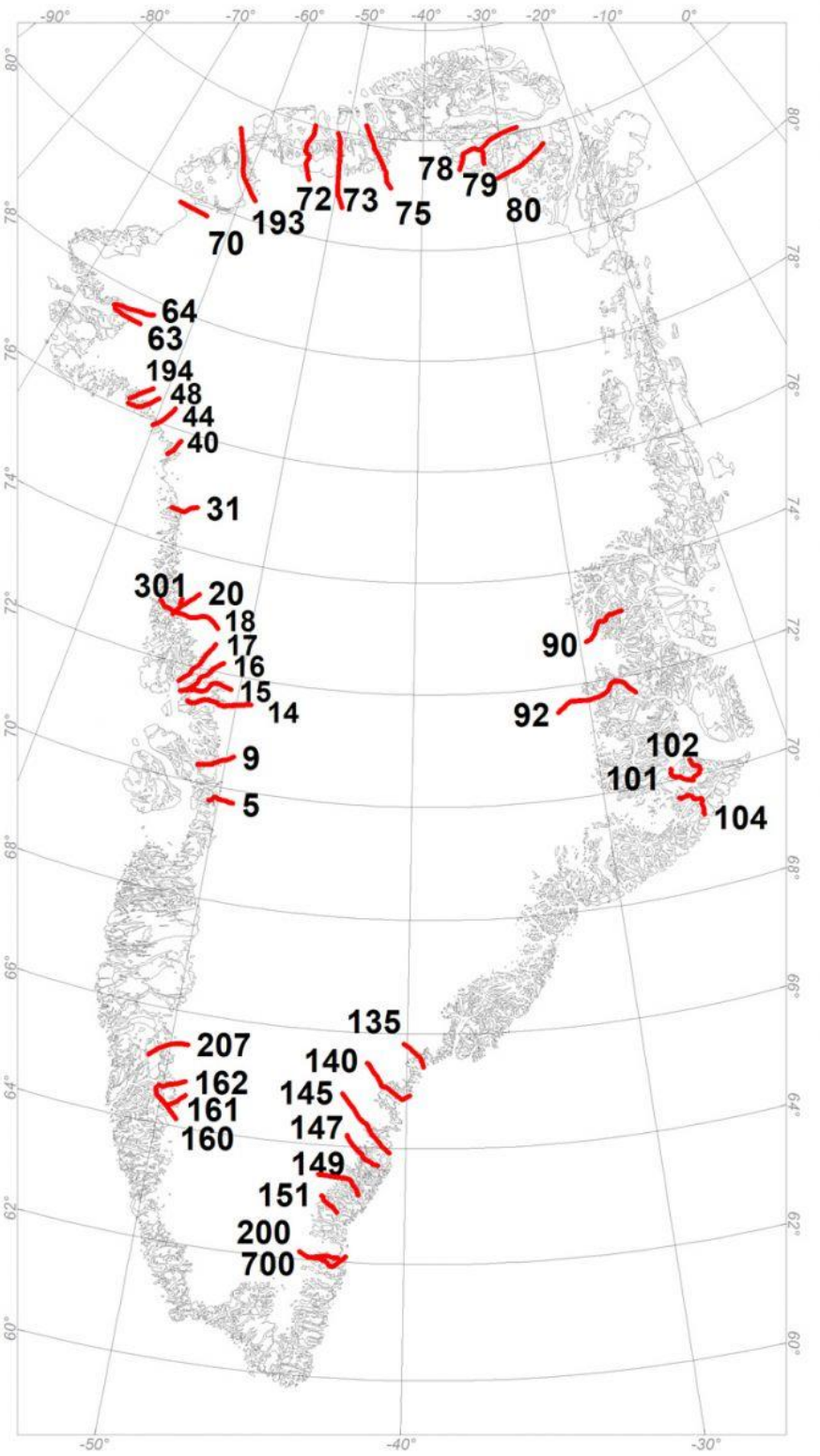

Figure 2. Greenland Glacier IDs

Table 3 lists the profiled Glacier IDs and names.

Table 3. Glacier IDs and Names

ID	Name	ID	Name
5	Eqip Sermia	90	Morell Gletscher
9	Store Gletscher	92	Daugaard-Jensen
14	Kangerlussuup Sermersua	101	Sydbrae
15	Rink Isbrae	102	Bredegletscher
16	Umiammakku Isbrae	104	Dendritgletscher
17	Inngia Isbrae	135	Ikertivaq N
18	Upernavik isstrom S	140	Koge Bugt C
20	Unnamed near Upernavik	145	Graulv
31	Alison Glacier	147	A.P. Bernstorff Gletscher
40	Sverdrup Glacier	149	Skinfaxe
44	Kong Oscar Glacier	151	Heimdal Gletscher
48	Rink Gletscher	160	Kangiata Nunaata Sermia
63	Heilprin Gletscher	161	Akullersuup Sermia
64	Tracy Gletscher	162	Narsap Sermia
70	Humboldt Glacier	193	Petermann Gletscher
72	Steensby Gletscher	194	Docker Smith Gl. W
73	Ryder Gletscher	200	Puisortoq N
75	C. H. Ostenfeld Gletscher	207	Nordenskiaeld Gletscher
78	Marie Sophie Gletscher	301	Unnamed near Upernavik
79	Academy Gletscher	700	Puisortoq S
80	Hagen brae		—

2 DATA ACQUISITION AND PROCESSING

2.1 Theory of Measurements

The gravity signal is extracted from an inertially based system in which a small mass is suspended within a magnetic field. Tiny variations in the acceleration of the gravimeter produce small electrical signals in the sensor as the mass moves within the magnetic field. The processed data from the AIRGrav instrument data consists of two data types: gravity and aircraft attitude.

2.2 Data Acquisition Methods

The gravimeter is located as near the airplane center of mass as possible. Simultaneously acquired gravimeter output GPS data are recorded on hard disks on the plane. Following the flight this data is downloaded onto a PC for processing.

2.3 Derivation Techniques and Algorithms

Inversion of the Greenland and Abbot gravity data for bathymetry was undertaken in two dimensions along individual flight lines using Geosoft GMSysTM software. The software performs iterative forward modeling using the technique of Talwani et al. (1959). The bed was kept fixed where it is observed in the radar data and the bathymetry in water-covered areas where the seafloor cannot be imaged with radar varied to obtain the best match to the observed gravity. The model is pinned to the observed gravity value at a location within the region where the bed can be observed.

2.3.1 Processing Steps

The following processing steps are performed by the data provider.

For all bathymetry data sets:

1. The gravimeter data were filtered and decimated to 10 Hz to match the GPS data.
2. GPS-derived accelerations were subtracted from the data.
3. The gravity was corrected for the Eötvös effect.
4. The expected gravity at the measurement latitude was subtracted.
5. The resulting anomalies were decimated to 2 Hz and low-pass filtered to suppress noise.
6. The free-air correction was applied.
7. After evaluating the noise level with different filter lengths, a 70 s filter was used. The filter half-wavelength is approximately 5 km at the average flight speed of 275 knots (142 m/s). Features narrower than the half wavelength can be resolved, but have an attenuated amplitude.
8. Horizontal accelerations associated with turns and other vigorous maneuvers disturb gravity measurements. A routine that examines horizontal accelerations was used to divide each flight into lines that are free of these perturbations.

For Greenland fjord and Abbot Ice Shelf data:

1. A forward model of gravity was generated according to Talwani (Talwani, 1959) with ice density 0.915 g/cc, water density 1.028 g/cc and rock density 2.67 g/cc. Ice surface and base are taken from the NASA Airborne Topographic Mapper (ATM) (Krabill, 2010) and the CReSIS Multichannel Coherent Radar Depth Sounder (MCoRDS) (Allen, 2009).
2. The model was pinned at a point where ice is grounded and nearby gravity variations are due only to variations in topography of the ice/rock interface. This establishes a DC shift to

relate the anomalies calculated for the model space to the anomalies measured on Earth. Where multiple lines were flown along approximately the same track, the same DC shift was applied.
3. A gravity inversion was performed on the water/rock interface under floating ice. This produced a model of the sub-ice shelf bathymetry responsible for the gravity anomaly.

For Northwest Greenland:

1. Data from survey lines were gridded by minimum curvature gridding with cell size of 500 m.
2. Gravity data were upward continued from survey elevation to a constant elevation of 2000 m above the ellipsoid.
3. A forward gravity model was built based on gridded data sets of surface, bed topography, and seafloor bathymetry (Bamber et al., 2013). A DC shift was established to match gravity values calculated within the model space to observed values. The value of the DC shift was established from the mean misfit between calculated and observed gravity over large islands and peninsulas along the coast.
4. The observed gravity was inverted for bathymetry in the software GMSys-3D, with algorithms based on Parker (1972).

3 VERSION HISTORY

On 11 February 2015, Version 1 was replaced by Version 1.1. The precision for latitude and longitude values in data file IGBTH4_20140207.csv was increased to six decimal places.

4 ERRORS AND LIMITATIONS

Errors range from ±50 m up to ±200 m in the Greenland data sets. The variability in uncertainty is largely due to profile length, with uncertainty increasing with distance from the pinning point usually near the grounding line. The main sources of error are from short-wavelength features, which are not modelled at full amplitude, and from the presence of either local variations in geology or long-wavelength regional geological variations. These have been accounted for in some cases, notably Petermann Glacier, where a regional correction to the observed gravity was applied in order to fit known bathymetric constraints at the end of the fjord (Johnston et al., 2011). Elsewhere, bathymetry inversion is not performed on gravity recovered from parts of fjords where magnetic anomalies indicate a significant change in rock type compared to the material at the point to which the model is pinned.

Errors are approximated as ±70 m for the Abbot data set, incorporating errors in gravity measurement, radar ice thickness, ATM surface elevation, 2-D model pinning point and some allowance for geological structures. Variations in bed density were incorporated utilizing rock outcrops as a guide. The model assumes the absence of sea floor sediments. If sea floor sediments are present the true bathymetry will be less deep than the model (Cochran et al., 2014).

5 SENSOR OR INSTRUMENT DESCRIPTION

The gravity instrument is a Sander AIRGrav designed for airborne applications. The AIRGrav system consists of a three-axis gyro-stabilized, Schuler-tuned inertial platform on which three orthogonal accelerometers are mounted. The primary gravity sensor is the vertical accelerometer that is held within 10 arc-seconds (0.0028 degree) of the local vertical by the inertial platform, monitored through the complex interaction of gyroscopes and two horizontal accelerometers (Sander et al., 2004). An advantage of the AIRGrav system over other airborne gravimeters is that it has been shown to be capable of collecting high-quality data during draped flights (Studinger et al., 2008). The gravimeter records accelerations arising from variations in the Earth's gravity field and accelerations experienced by the airplane. These accelerations are recorded at 128 Hz. Aircraft accelerations are obtained utilizing differential GPS measurements.

6 REFERENCES

Bamber et al. 2013. A New Bed Elevation Data set for Greenland. The Cryosphere, 7:499-510.

Leuschen, Carl, and Chris Allen. 2010, updated 2014. IceBridge MCoRDS L2 Ice Thickness. Boulder, Colorado USA: National Snow and Ice Data Center. http://nsidc.org/data/irmcr2.html.

Cochran, J. R., S. S. Jacobs, K. J. Tinto, and R. E. Bell. 2014. Bathymetric and Oceanic Controls on Abbot Ice Shelf Thickness and Stability, The Cryosphere, 8:877-889, doi:10.5194/tc-8-877-2014.

Cochran, J. R., S. S. Jacobs, K. J. Tinto, and R. E. Bell. 2014. Supplement of Bathymetric and oceanic controls on Abbot Ice Shelf thickness and stability, The Cryosphere, 8, 877-889, doi:10.5194/tc-8-877-2014-Supplement.

Forste, C., R. Schmidt, R. Stubenvoll, F. Flechtner, U. Meyer, R. Konig, H. Neumayer, R. Biancale, J. M. Lemoine, S. Bruinsma, S. Loyer, F. Barthelmes, and S. Esselborn. 2008. The GeoForschungsZentrum Potsdam/Groupe de Recherche de Geodesie Spatiale Satellite-only and Combined Gravity Field Models: Eigen-GL04S1 and Eigen-GL04C, Journal of Geodesy, 82:331-346, doi:10.1007/s00190-007-0183-8.

Fretwell, P., H. D. Pritchard, D. G. Vaughan, J. L. Bamber, N. E. Barrand, R. E. Bell, C. Bianchi, R. G. Bingham, D. D. Blankenship, G. Casassa, G. A. Catania, D. Callens, H. Conway, A. J. Cook, H. F. J. Corr, D. Damaske, V. Damm, F. Ferraccioli, R. Forsberg, K. Fujita, Y. Gim, P. Gogineni, D. J. Griggs, R. C. A. Hindmarsh, P. Holmlund, J. W. Holt, R. W. Jacobel, A. Jenkins, W. Jokat, T. A. Jordan, E. C. King, J. Kohler, W. Krabill, M. Riger-Kusk, K. Langley, G. Leitchenkov, C. Leuschen, B. P. Luyendyk, K. Matsuoka, J. Mouginot, F. O. Nitsche, Y. Nogi, O. A. Nost, S. V. Popov, E. Rignot, D. M. Rippin, A. Rivera, J. L. Roberts, N. Ross, M. J. Siegert, A. M. Smith, D. Steinhage, M. Studinger, B. Sun, K. J. Tinto, B. C. Welch, D. S. Wilson, D. A. Young, C. Xiangbin, and A.

Zirizzotti. 2013. Bedmap2: Improved Ice Bed, Surface and Thickness Datasets for Antarctica, The Cryosphere, 7:375-393, doi:10.5194/tc-7-375-2013.

Johnson, H.L., A. Münchow, K. K. Falkner, and H. Melling. 2011. Ocean Circulation and Properties in Petermann Fjord, Greenland. Journal of Geophysical Research: Oceans, 116:C01003, doi:10.1029/2010JC006519.

Krabill, William B. 2010, updated 2014. IceBridge ATM L2 Icessn Elevation, Slope, and Roughness. Version 2. Boulder, Colorado USA: NASA DAAC at the National Snow and Ice Data Center. http://nsidc.org/data/ilatm2.html.

Parker, R. L. 1972. The Rapid Calculation of Potential Anomalies. Geophysical Journal of the Royal Astronomical Scoiety, 42:315-334.

Sander, S., M. Argyle, S. Elieff, S. Ferguson, V. Lavoie, and L. Sander. 2004. The AIRGrav Airborne Gravity System, in Airborne Gravity 2004 - Australian Society of Exploration Geophysicists Workshop, edited by R. Lane, pp. 49-53, Geoscience Australia, http://www.ga.gov.au/image_cache/GA16642.pdf.

Studinger, M., R. E. Bell, and N. Frearson. 2008. Comparison of AIRGrav and GT-1A Airborne Gravimeters for Research Applications, Geophysics, 73: 151-161.

Talwani, M., J. L.Worzel, and M. Landisman. 1959. Rapid Gravity Computations for Two-dimensional Bodies with Application to the Mendocino Submarine Fracture Zone, Journal of Geophysical Research, 64(1):49-59.

7 RELATED DATA COLLECTIONS

- IceBridge Sander AIRGrav L1B Geolocated Free Air Gravity Anomalies
- IceBridge Sander AIRGrav L3 Bathymetry

8 DOCUMENT INFORMATION

8.1 Publication Date

October 2014

8.2 Date Last Updated

March 2025